Adaptive Central-Upwind Scheme on Triangular Grids for the Saint-Venant System

Yekaterina Epshteyn and Thuong Nguyen

THE UNIVERSITY OF UTAH

Abstract

In this work, we develop a robust adaptive well-balanced and positivity-preserving central-upwind scheme on unstructured triangular grids for shallow water equations. The numerical method is an extension of the scheme from [Liu *et al.*,J. of Comp. Phys, 374 (2018), pp. 213 - 236]. As a part of the adaptive central-upwind algorithm, we obtain local a posteriori error estimator for the efficient mesh refinement strategy. The accuracy, high-resolution and efficiency of new adaptive central-upwind scheme are demonstrated on a number of challenging tests for shallow water models.

2D Shallow Water Equation

We consider the two-dimensional (2-D) Saint-Venant system of shallow water equations:

$$h_t + (hu)_x + (hv)_y = 0,$$
$$(hu)_t + (hu^2 + \frac{1}{2}gh^2)_x + (huv)_y = -ghB_x,$$
$$(hv)_t + (huv)_x + (hv^2 + \frac{1}{2}gh^2)_y = -ghB_y.$$

In vector form as a balance law:

$$\mathbf{U}_t + \mathbf{F}(\mathbf{U}, B)_x + \mathbf{G}(\mathbf{U}, B)_y = \mathbf{S}(\mathbf{U}, B).$$

Notation

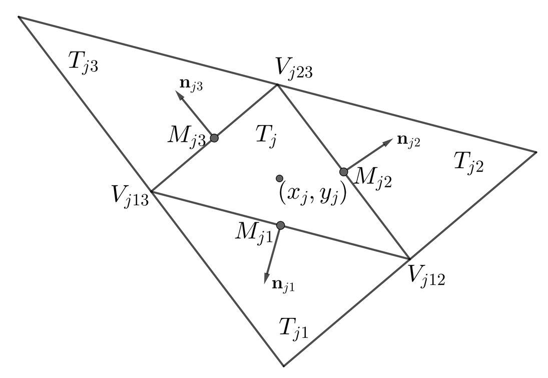

Figure 1: Triangular cell with neighbors.

Second-Order High-Resolution Central-Upwind Schemes

The cell average for T_j

$$\bar{\mathbf{U}}_j(t) \approx \frac{1}{|T_j|} \iint_{T_j} \mathbf{U}(x, y, t) dxdy$$

$$\frac{d\bar{\mathbf{U}}_j}{dt} = -\frac{1}{|T_j|}[\mathbf{H}_{j1} + \mathbf{H}_{j2} + \mathbf{H}_{j3}] + \bar{S}_j,$$

where the cell-average of the source term:

$$\bar{\mathbf{S}}_j(t) \approx \frac{1}{|T_j|} \iint_{T_j} S(\mathbf{U}(x, y, t), B(x, y)) dxdy$$

and the numerical fluxes through the corresponding edges of the triangle T_j are

$$\begin{aligned}\mathbf{H}_{jk} = &\frac{l_{jk} cos(\theta_{jk})}{a^{in}_{jk} + a^{out}_{jk}} \left[a^{in}_{jk}\mathbf{F}(\mathbf{U}_{jk}(M_{jk}), B_{jk}) + a^{out}_{jk}\mathbf{F}(\mathbf{U}_j(M_{jk}), B_{jk})\right] \\ &+ \frac{l_{jk} sin(\theta_{jk})}{a^{in}_{jk} + a^{out}_{jk}} \left[a^{in}_{jk}\mathbf{G}(\mathbf{U}_{jk}(M_{jk}), B_{jk}) + a^{out}_{jk}\mathbf{G}(\mathbf{U}_j(M_{jk}), B_{jk})\right] \\ &- l_{jk}\frac{a^{in}_{jk} a^{out}_{jk}}{a^{in}_{jk} + a^{out}_{jk}} \left[\mathbf{U}_{jk}(M_{jk}) - \mathbf{U}_j(M_{jk})\right], k = 1, 2, 3\end{aligned}$$

The pointwise value of the solution in triangle T_j is approximated by second-order piecewise linear reconstruction:

$$\tilde{\mathbf{U}}_j(x, y) = \bar{\mathbf{U}}_j + (\mathbf{U}_x)(x - x_j) + (\mathbf{U}_y)(y - y_j)$$

Discontinuities appearing in the reconstruction step at the cell interfaces, propagate at finite speeds in the direction $\pm n_{jk}$ are estimated by a^{in}_{jk}, a^{out}_{jk}:

$$a^{in}_{jk} = -min\{\lambda_-[J_{jk}(\mathbf{U}_j(M_{jk}))], \lambda_-[J_{jk}(\mathbf{U}_{jk}(M_{jk}))], 0\},$$
$$a^{out}_{jk} = max\{\lambda_+[J_{jk}(\mathbf{U}_j(M_{jk}))], \lambda_+[J_{jk}(\mathbf{U}_{jk}(M_{jk}))], 0\},$$

where $\lambda_-[J_{jk}]$, $\lambda_+[J_{jk}]$ are the smallest and largest eigenvalues of the Jacobi matrix $J_{jk} = \cos(\theta_{jk})\frac{\partial \mathbf{F}}{\partial \mathbf{U}} + \sin(\theta_{jk})\frac{\partial \mathbf{G}}{\partial \mathbf{U}}$

Well-Balanced and Positivity-Preserving Central-Upwind Scheme

Main ideas of the scheme proposed in [2]:

- Replace the variable h by $w := h + B$ in the shallow water equations.
- The bottom topography $B(x, y)$ is approximated using a continuous piecewise linear interpolation.
- Define three type of computational cells: fully flooded, partially flooded, and dry.
- A first-order water surface reconstruction conserves mass and preserves the positivity and well-balanced properties for "dry lake" steady states.
- Introduce second-order well-balanced reconstruction to correct the water depth in partially flooded triangles

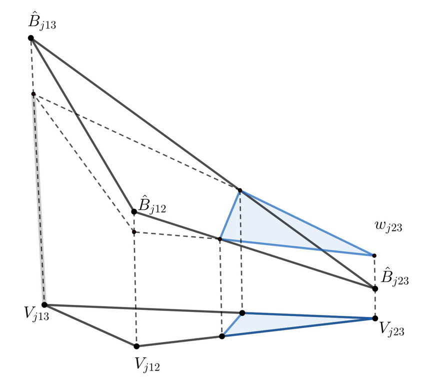

Figure 2: Second order reconstruction for partially flooded cell

- The "draining" time-step method is derived in order to have the positivity of water depth.

$$\bar{\mathbf{U}}^{n+1}_j = \bar{\mathbf{U}}^n_j - \frac{1}{|T_j|}\sum_{k=1}^{3} \Delta t^{drain}_{jk} \mathbf{H}_{jk} + \Delta t \bar{S}_j$$

- A new quadrature for the source term is developed that maintain the well-balanced property of the scheme.

Adaptive Central-Upwind Scheme

The adaptive central-upwind algorithm is described briefly by the following steps, see [1].

Step 0. At time $t = t^0$, generate the initial uniform grid $\mathcal{T}^{0,0}$.
Step 1. On mesh $\mathcal{T}^{n,\mathcal{M}_n}$, evolve the cell averages $\bar{\mathbf{U}}^n$ to $\bar{\mathbf{U}}^{n+1}$ using the second-order adaptive time evolution.
Step 2. On mesh $\mathcal{T}^{n,\mathcal{M}_n}$, compute WLR error and update the refinement/de-refinement status for each cell/triangle.
Step 3. Generate the new adaptive mesh $\mathcal{T}^{n+1,\mathcal{M}_{n+1}}$ at t^{n+1}.
Step 4. Repeat **Step 1** - **Step 3** until final time.

Adaptive Mesh Refinement/Coarsening

Goal: Design an efficient local mesh refinement procedure.

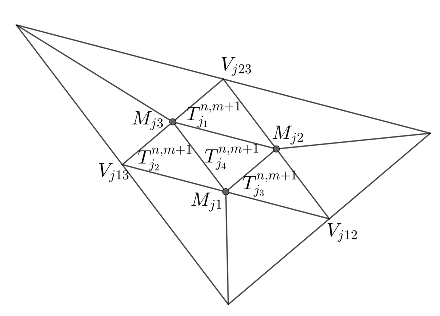

Figure 3: Refinement in fully flooded cells

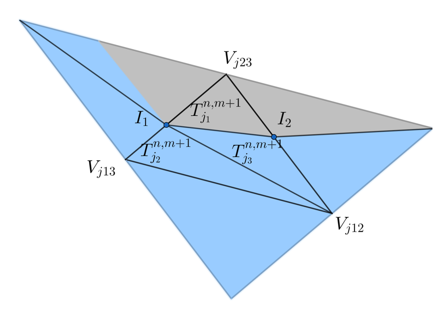

Figure 4: Refinement in partialy flooded cells

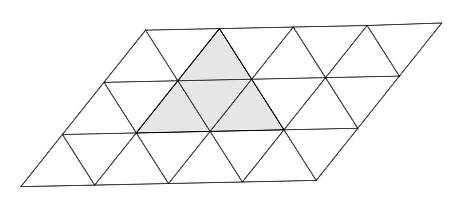

Figure 5: Coarse mesh $\mathcal{T}^{n,0}$

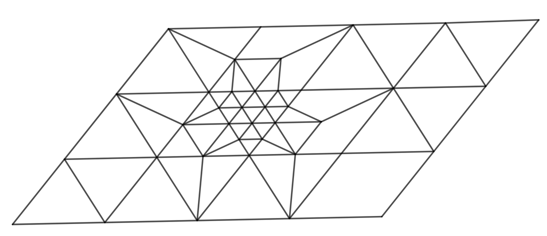

Figure 6: Adaptive mesh $\mathcal{T}^{n,2}$

Error estimator:

Using the idea of Weak Local Residual (WLR) from [3] and [4], we have derived local error estimator in [1] that is used as the robust indicator for the adaptive mesh refinement on triangular mesh. At each node N_i, we compute the error $E^{n+\frac{1}{2}}_i$ by

$$E^{n+\frac{1}{2}}_i = \frac{1}{\Delta}(\mathcal{U}^{n+\frac{1}{2}}_i + \mathcal{F}^{n+\frac{1}{2}}_i + \mathcal{G}^{n+\frac{1}{2}}_i),$$
$$\mathbf{U}^{n+\frac{1}{2}}_i = \sum_{c=1}^{C_i} \frac{1}{3}|T^{n,\mathcal{M}_n}_{j_c}|(\bar{w}^n_{j_c} - \bar{w}^{n+1}_{j_c}),$$
$$\mathcal{F}^{n+\frac{1}{2}}_i = \sum_{c=1}^{C_i} a^{(i)}_c \frac{\Delta t}{2}|T^{n,\mathcal{M}_n}_{j_c}|((\bar{hu})^n_{j_c} + (\bar{hu})^{n+1}_{j_c}),$$
$$\mathcal{G}^{n+\frac{1}{2}}_i = \sum_{c=1}^{C_i} b^{(i)}_c \frac{\Delta t}{2}|T^{n,\mathcal{M}_n}_{j_c}|((\bar{hv})^n_{j_c} + (\bar{hv})^{n+1}_{j_c}).$$

The error in a cell $T^{n,\mathcal{M}_n}_j \in \mathcal{T}^{n.\mathcal{M}_n}$ is given by,

$$e_j = \max_{\kappa} \left|E^{n+\frac{1}{2}}_{jk}\right|, \quad \kappa = 12, 23, 13,$$

where $E^{n+\frac{1}{2}}_{j\kappa}$ is the WLR error computed at node $V_{j\kappa}$ of T_j. The error e_j in each cell $T^{n.\mathcal{M}_n}_j \in \mathcal{T}^{n,\mathcal{M}_n}$ is compared to an error tolerance, and the cell is either "flagged" for refinement/de-refinement or "no-change".

Second-order Adaptive Time Evolution

An adaptive stepsize algorithm in [1] is applied for the adaptive mesh to evolve from t^n to next time level as follows.

- Group all cells $T^{n,\mathcal{M}_n}_j \in \mathcal{T}^{n,\mathcal{M}_n}$ in cell levels $l = 0, 1, .., L$ based on their sizes.
- Calculate the reference time step Δt and the local time step for each cell level.
- On each cell $T^{n,\mathcal{M}_n}_j$ of level l, for each substep $[t^{n,p}_l, t^{n,p+1}_l], p = 0, 1, ..., \mathcal{P}_l - 1$, we apply the following two adaptive steps of SSPRK2 method,

$$\bar{\mathbf{U}}^{(1)}_j = \bar{\mathbf{U}}^{n,p}_j - \frac{1}{|T^{n,\mathcal{M}_n}_j|}\sum_{k=1}^{3} \Delta t^{n,p}_{jk} \mathbf{H}^{n,p}_{jk} + \Delta t^{n,p}_l \bar{\mathbf{S}}^{n,p}_j := \mathbf{R}(\bar{\mathbf{U}}^{n,p}_j, \Delta t^{n,p}_l),$$
$$\bar{\mathbf{U}}^{n,p+1}_j = \frac{1}{2}\bar{\mathbf{U}}^{n,p}_j + \frac{1}{2}\mathbf{R}(\bar{\mathbf{U}}^{(1)}_j, \Delta t^{n,p}_l)$$

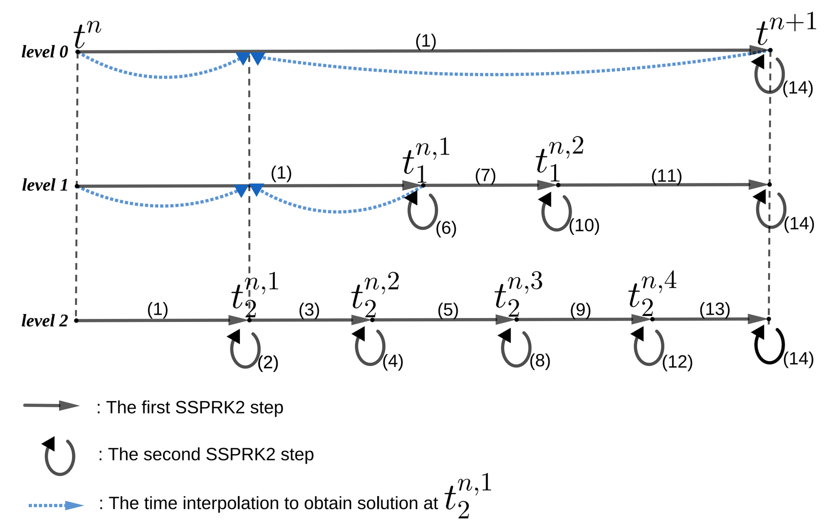

Figure 7: The example of SSPRK2 on mesh with three cell levels, $l = 0, 1, 2$.

Numerical Results

Example of the small perturbation steady-state problem in [1]
Bottom Topography:

$$B(x, y) = \begin{cases} 1.1, & r \leq 0.1, \\ 11(0.2 - r) & 0.1 < r \leq 0.2, \\ 0, & \text{otherwise,} \end{cases} \quad r := \sqrt{(x - 0.5)^2 + (y - 0.5)^2}.$$

Initial condition:

$$w(x, y, 0) = \begin{cases} 1 + 0.01, & 0.1 < x < 0.2, \\ \max(1, B(x, y)), & \text{otherwise,} \end{cases} \quad u \equiv v \equiv 0,$$

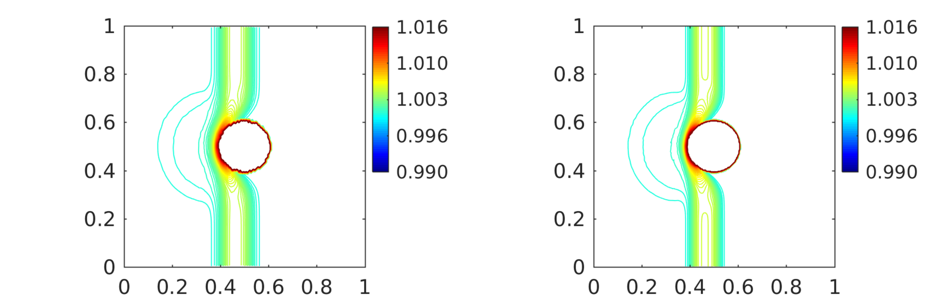

Figure 8: w component of the solution of the IVP computed by the central-upwind scheme on uniform triangular meshes 2*100*100 (left plot) and 2*200*200 (right plot) at $t = 0.1$.

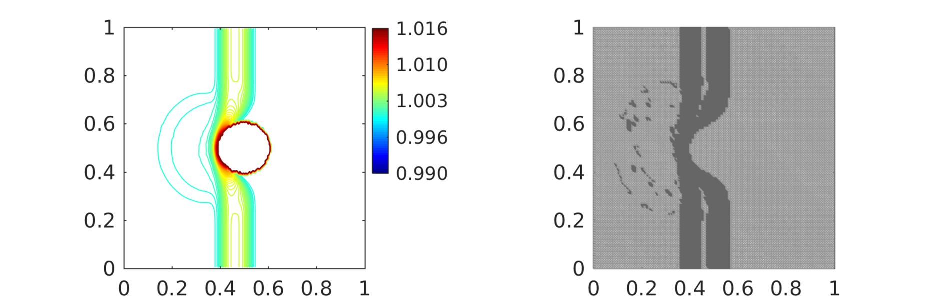

Figure 9: w component of the solution of the IVP computed by **the adaptive central-upwind scheme** on triangular meshes 2*100*100 (left plot) and the adaptive mesh (right plot) at $t = 0.1$.

uniform mesh (cells)	adaptive mesh $\mathcal{M} = 1$ (cells)	$\mathcal{R}_{CPU}$ with $\mathcal{M} = 1$	adaptive mesh $\mathcal{M} = 2$ (cells)	$\mathcal{R}_{CPU}$ with $\mathcal{M} = 2$
$2 \times 100 \times 100$	11,831	1.91	6,155	3.04
$2 \times 200 \times 200$	31,050	2.08	25,753	3.14
$2 \times 400 \times 400$	154,616	3.16	94,357	5.82
$\mathcal{R}_{CPU}$ average:		2.38		4.00

Table 1: The R_{CPU} ratio at $t = 0.1$, where $\mathcal{R}_{CPU} = \frac{CPU_{uniform}}{CPU_{adaptive}}$ is the ratio of the CPU times of the central-upwind algorithm without adaptivity to the CPU time of the adaptive central-upwind algorithm (uniform mesh and the compared adaptive mesh have the same size of the smallest cells).

Conclusion and Future Work:

- Adaptive mesh refinement produces higher resolution at smaller computational cost.
- Goal: test and apply adaptive central-upwind schemes for a variety of shallow water models.

References

[1] Yekaterina Epshteyn and Thuong Nguyen, *Adaptive Central-Upwind Scheme on Triangular Grids for the Saint-Venant System*, Manuscript submitted for publication.

[2] X. Liu, J. Albright, Y. Epshteyn, and A. Kurganov, *Well-balanced positivity pre- serving central-upwind scheme with a novel wet/dry reconstruction on triangular grids for the Saint-Venant system*, Journal of Computational Physics, 374 (2018), pp. 213-236.

[3] S. Karni and A. Kurganov, *Local error analysis for approximate solutions of hyperbolic conservation laws*, Adv. Comput. Math., 22 (2005), pp. 79-99.

[4] E. Tadmor, *Local error estimates for discontinuous solutions of nonlinear hyperbolic equations*, SIAM J. Numer. Anal., 28 (1991), pp. 891-906.